

A composite micromotor driven by self-thermophoresis and Brownian rectification

Xin Lou(娄辛), Nan Yu(余楠), Ke Chen(陈科), Xin Zhou(周昕), Rudolf Podgornik, and Mingcheng Yang(杨明成)

Citation: Chin. Phys. B, 2021, 30 (**11**): 114702. DOI: 10.1088/1674-1056/ac2727
Journal homepage: http://cpb.iphy.ac.cn; http://iopscience.iop.org/cpb

What follows is a list of articles you may be interested in

Molecular dynamics simulation of thermal conductivity of silicone rubber

Wenxue Xu(徐文雪), Yanyan Wu(吴雁艳), Yuan Zhu(祝渊), Xin-Gang Liang(梁新刚)
Chin. Phys. B, 2020, 29 (**4**): 046601. DOI: 10.1088/1674-1056/ab7743

Radial transport dynamics studies of SMBI with a newly developed TPSMBI code

Ya-Hui Wang(王亚辉), Wen-Feng Guo(郭文峰), Zhan-Hui Wang(王占辉), Qi-Long Ren(任启龙), Ai-Ping Sun(孙爱萍), Min Xu(许敏), Ai-Ke Wang(王爱科), Nong Xiang(项农)
Chin. Phys. B, 2016, 25 (**10**): 106601. DOI: 10.1088/1674-1056/25/10/106601

Surface-charge-governed electrolyte transport in carbon nanotubes

Xue Jian-Ming, Guo Peng, Sheng Qian
Chin. Phys. B, 2015, 24 (**8**): 086601. DOI: 10.1088/1674-1056/24/8/086601

Molecular dynamics study of thermal stress and heat propagation in tungsten under thermal shock

Fu Bao-Qin, Lai Wen-Sheng, Yuan Yue, Xu Hai-Yan, Li Chun, Jia Yu-Zhen, Liu Wei
Chin. Phys. B, 2013, 22 (**12**): 126601. DOI: 10.1088/1674-1056/22/12/126601

RAPID COMMUNICATION

A composite micromotor driven by self-thermophoresis and Brownian rectification*

Xin Lou(娄辛)[1,2], Nan Yu(余楠)[1,2,3], Ke Chen(陈科)[1,2,4], Xin Zhou(周昕)[1,5], Rudolf Podgornik[1,2,5,†], and Mingcheng Yang(杨明成)[1,2,4,‡]

[1] *University of Chinese Academy of Sciences, Beijing* 100049, *China*
[2] *Beijing National Laboratory for Condensed Matter Physics and Key Laboratory of Soft Matter Physics, Institute of Physics, Chinese Academy of Sciences, Beijing* 100190, *China*
[3] *Institute for Advanced Study, Shenzhen University, Shenzhen* 518060, *China*
[4] *Songshan Lake Materials Laboratory, Dongguan* 523808, *China*
[5] *Wenzhou Institute, University of Chinese Academy of Sciences, Wenzhou* 325001, *China*

(Received 17 August 2021; revised manuscript received 6 September 2021; accepted manuscript online 16 September 2021)

Brownian motors and self-phoretic microswimmers are two typical micromotors, for which thermal fluctuations play different roles. Brownian motors utilize thermal noise to acquire unidirectional motion, while thermal fluctuations randomize the self-propulsion of self-phoretic microswimmers. Here we perform mesoscale simulations to study a composite micromotor composed of a self-thermophoretic Janus particle under a time-modulated external ratchet potential. The composite motor exhibits a unidirectional transport, whose direction can be reversed by tuning the modulation frequency of the external potential. The maximum transport capability is close to the superposition of the drift speed of the pure Brownian motor and the self-propelling speed of the pure self-thermophoretic particle. Moreover, the hydrodynamic effect influences the orientation of the Janus particle in the ratched potential, hence also the performance of the composite motor. Our work thus provides an enlightening attempt to actively exploit inevitable thermal fluctuations in the implementation of the self-phoretic microswimmers.

Keywords: Brownian motors, self-phoretic microswimmers, thermal noise, hydrodynamic effect

PACS: 47.57.–s, 66.10.cd, 02.70.Ns **DOI:** 10.1088/1674-1056/ac2727

1. Introduction

Active matter consists of units that individually convert environmental or stored energy into self-propulsion or mechanical force[1] — as is the case for motor proteins, bacteria and artificial active colloidal particles — becoming a fascinating subject of nonequilibrium physics and micro-/nanotechnology. Due to intrinsically out-of-equilibrium features, active matter often exhibits exotic phenomena that are unattainable in equilibrium systems, including the motility-induced phase transition, abnormal rheology as well as emergent collective behavior.[2–7] Generally, microscale active units are also called micromotors in order to highlight their similarities with macroscopic motors. In terms of the inevitable thermal and/or other types of noise, micromotors can be roughly classified into Brownian motor type and self-propelled active particle type, for whose performances the effect of the noise is positive and negative, respectively.

Brownian motors refer to submicron-scale machines, which can utilize — but do not necessarily have to — noise combined with unbiased external input signals to achieve a directed motion in asymmetric rachet potentials,[8–13] such as biological ion pumps and bio-molecular motors.[14–19] When the external ratchet potential is time-modulated to alternately switch on and off, such microdevices are termed pulsated-ratchet-type Brownian motors.[12] The interplay between the time-modulated ratchet potential and noise generates a directed drift without any net external force. On the other hand, self-propelled active particles generate a driving force along their inherent axis through different physical and chemical effects such as non-reciprocal shape change, bubble release or self-phoresis. Prominent examples would include biological microorganisms[20,21] and artificial active Janus colloids.[22–28] In these cases the external ratchet potential is absent and the noise only disturbs the persistent directed swimming motion of the active particle, randomizing its trajectory. Consequently, the self-propelled particles behave like effective Brownian particles at long timescales. The thermal noise is in this case thus not conducive to the operation of the self-propelled active particles, demanding an extra steering strategy to achieve a directed transport on large length scales.

Given the negative effect of thermal fluctuations on the self-propelled particle, an interesting issue emerges, whether

*Project supported by the National Natural Science Foundation of China (Grant Nos. 11874397 and 11674365).
†Corresponding author. E-mail: rudipod@gmail.com
‡Corresponding author. E-mail: mcyang@iphy.ac.cn
© 2021 Chinese Physical Society and IOP Publishing Ltd

the self-propelled particle can actively exploit thermal noise to improve its performance? Inspired by the Brownian motor, a possible and straightforward scheme would be to construct a composite micromotor by combining the self-propelled particle with the Brownian ratchet. Such a composite motor could possess features of both, the self-propelled particle as well as the Brownian motor. Recently, static asymmetric external fields or boundary walls have been employed to regulate the motion of the self-propelled particles,[29–31] although these designs still correspond to a Brownian motor, in which the active motion acts like an input signal. More recently, rectification of active Brownian particles by a time-oscillating potential has been numerically investigated,[32] with the self-propulsion artificially imposed rather than arising naturally from a physical process. In addition, the hydrodynamic effects have not been taken into account in this case.

In the present work, based upon the mesoscale fluid simulations, we investigate the transport of a two-dimensional self-thermophoretic Janus particle in a time-modulated dynamic ratchet potential, amounting to a composite motor formed from the pulsated-ratchet Brownian motor and the self-phoretic active particle. This composite motor exhibits a directed transport, where thermal noise is actively exploited due to the time-modulated ratchet potential. By extensively exploring the parameter space, we show that the transport velocity of the Janus particle depends sensitively on the modulated frequency of the external potential. Furthermore, the mesoscale simulation method used in the work allows us to study the hydrodynamic effects on the orientation of the active Janus particle and hence its transport, exhibiting a significant polarization of the self-thermophoretic Janus particle in direct contrast to the case of the active Brownian particle.

2. Simulation method and systems

2.1. Solvent

In order to bridge the large gap in the time and length scales between the colloidal and the solvent particles, we employ a two-dimensional hybrid simulation scheme. The solvent is modeled by a particle-based mesoscale approach known as multiparticle collision dynamics (MPC),[33–36] while the colloid particle is described by a standard molecular dynamics (MD) method. In the MPC approach, the fluid is represented by N point particles, each with a mass m, position r_i, and velocity v_i, with $1 < i < N$. The particle dynamics consists of alternating streaming and collision steps. In the streaming step, all the solvent particles move ballistically for a time h. In the collision step, the particles are sorted into a square lattice with lattice size a, and interchange momentum relative to the center-of-mass velocity of each collision cell. In our simulations we use the stochastic rotational collision rule with variable collision angle α, as introduced by Ryder and Yeomans.[36,37] This collision rule locally conserves mass, linear momentum, energy and angular momentum. To guarantee the Galilean invariance, the grid of collision cells is also randomly shifted before each collision step. The coarse-grained method correctly captures hydrodynamic interactions, mass transport, heat conduction and thermal fluctuations. Simulation units are reduced by setting $a = 1$, $m = 1$, and the system mean temperature $k_B\overline{T} = 1$ with k_B the Boltzmann constant. We employ standard MPC parameters $h = 0.1$ and the mean number of solvent particles per cell $\rho = 10$.

2.2. Self-thermophoretic Janus particle

The colloidal particle is modeled by a single bead that interacts with the solvent via a Lennard–Jones (LJ)-type potential

$$U(r) = 4\varepsilon\left[\left(\frac{\sigma}{r}\right)^{2k} - \left(\frac{\sigma}{r}\right)^{k}\right], \quad r \le r_c \tag{1}$$

with the potential intensity $\varepsilon = 1$, the colloidal particle radius $\sigma = 4.0$, and the positive integer $k = 14$, which controls the potential stiffness. Here, r is the distance from the bead center to the solvent, with $r_c = 5.3$ the cutoff distance. The Janus particle is constructed by defining a body-fixed orientation vector $\boldsymbol{n}$ (symmetry axis), with its two hemispheres having different physical properties. The forward hemisphere (with the polar angle $\theta \le \pi/2$ with respect to $\boldsymbol{n}$, Fig. 1(a)) is modeled as the heated hemisphere by using local thermostats to heat its surrounding solvent.[38–40] Briefly, the thin layer of fluid around the forward hemisphere is divided into several small areas. For each area, the thermal kinetic energy of solvent is improved by rescaling their velocities relative to the center-of-mass velocity of the element. Outside the thin layer, the energy is locally conserved so that the heat conduction process is physically correct. Experimentally, the Janus particle can heat the surronding solvent under an illumination by coating a light-absorbing material on its heated hemisphere.[26] The input energy is drained from the system by fixing the mean temperature of the solution to a lower value, which is realized by uniformly rescaling the velocities of all the fluid particles relative to the solvent center-of-mass velocity. Since the system is large, this operation hardly affects the particle dynamics. The resulting temperature field is consequently compatible with the heat diffusion equation.

The MPC solvent has an ideal gas equation of state, so the solvent density is lower around the heated hemisphere than the non-heated one. The larger number of particles on the non-heated side produces a stronger attraction. Consequently, the Janus particle self-propels towards the low temperature area, namely, against the $\boldsymbol{n}$ axis. Moreover, in order to model the rotational diffusion of the colloidal parti-

cle, a sticky boundary condition is implemented on the particle surface through a revised bounce-back collision rule.[40] With the system parameters employed in the mesoscale simulation, the self-thermophoretic Janus particle has the self-propelled velocity $v_s = 0.018$, the rotational diffusion coefficient $D_r = 0.0038$, and the translational diffusion coefficient $D_t = 0.015$. The simulation box is a rectangle with dimensions $L_x \times L_y = 102 \times 40$, where the periodic boundary condition and the stick wall are applied in the x and y directions, respectively.

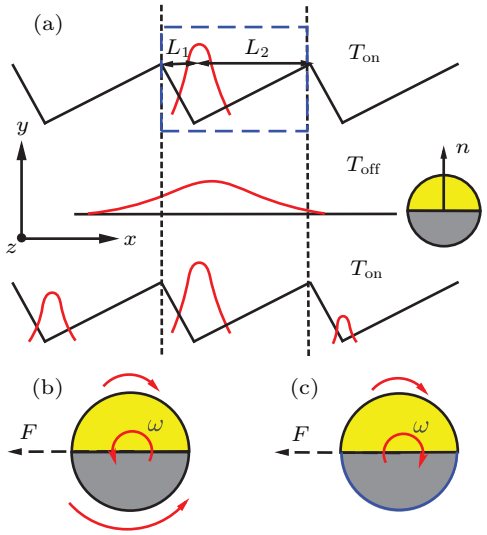


Fig. 1. (a) Schematic diagram of a self-thermophoretic Janus particle in an asymmetric external ratchet potential characterized by two length scales L_1 and L_2. The self-thermophoretic Janus particle self-propells against its heated side (yellow hemisphere). The red curves sketch the spatial probability distribution of the active particle with the ratchet potential off or on. (b), (c) Hydrodynamic alignment of the self-thermophoretic Janus particles, moving in the x-direction, induced by asymmetric surface friction (red arrows): (b) corresponds to the case of the stick boundary for the whole particle surface, while (c) corresponds to the slip boundary at the nonheated surface (blue line).

2.3. External ratchet potential

In order to model the pulsated Brownian ratchet that utilizes thermal noise, an external sawtooth-like potential $V(x)$ is applied to the active Janus particle, with a spatial period $L = 5.1$ that is comparable to the persistent length of the self-thermophoretic particle. The external potential is spatially asymmetric by skewing the barriers to the right with different ratchet lengths $L_1 = 0.71$ and $L_2 = 4.39$, as sketched in Fig. 1(a). The ratchet potential is constructed in a piecewise manner, with both the potential and its first-order derivative being continuous. Within a repeated unit, the force applied on the colloidal particle due to the ratchet potential has the form

$$F(x) = \begin{cases} 30, & x \in [0.0, 0.4), \\ -17\sin[5\pi(x-0.5)] + 13, & x \in [0.4, 0.6), \\ -4, & x \in [0.6, 4.9), \\ -17\sin[5\pi(x-5.2)] + 13, & x \in [4.9, 5.1]. \end{cases}$$

The ratchet potential is time modulated by periodically turning it on and off, with residence time T_{on} in the on state and T_{off} in the off state ($T_{tot} = T_{on} + T_{off}$ the modulation period). The strength of the external ratchet force is stronger than the self-thermophoretic force on the Janus particle, $F_s = k_B T v_s / D_t$, so that the active Janus particle stays in a close vicinity of the potential minima when the ratchet potential is on.

3. Results and discussion

3.1. Brownian motor with a passive colloidal particle

We first use the mesoscale fluid method to simulate a traditional Brownian motor, with a passive colloidal particle subjected to a periodically varying ratchet potential. Figure 2(a) displays the contour plot of the transport velocity of the Brownian motor, showing that the passive colloidal particle moves to the left (i.e., toward the steeper potential side) in the range of parameters under study. This result is consistent with the standard pulsated-type Brownian motor[41–43] and can be well understood accordingly. Briefly, when the ratchet potential is on, the passive colloidal particle basically stays in close vicinity of potential minima because the depth of the potential well is much larger than $k_B T$. When the ratchet potential is off, the particle can diffuse freely with a relatively larger probability, crossing the area corresponding to its left-side barrier (the short edge of the sawtooth potential). Consequently, the passive colloidal particle drifts with a negative velocity. The transport velocity is found to sensitively depend on the modulation period T_{tot} and the residence time T_{on}. Within an optimal range of T_{on} and T_{tot}, the Brownian motor can achieve a maximum transport velocity around -0.018. This optimal performance can be easily understood by noticing that for small T_{tot} or large T_{on} the passive particle is difficult to diffuse across the barrier region, while for long T_{tot} or short T_{on} the ratchet potential hardly plays a role.

For comparison, we also performed overdamped Brownian dynamics simulations to calculate the contour plot of the Brownian motor transport velocity (Fig. 2(b)), in which the particle diffusion coefficients are imposed to be the same as those in the mesoscale fluid simulation. It is found that the absence of hydrodynamic effects can largely change the transport velocity map of the Brownian micromotor. Particularly, in this case, the optimal transport parameters (T_{on} and T_{tot}) are different from those in the case of the mesoscale fluid simulation.

3.2. Composite micromotor with a self-thermophoretic particle

In this section, we model a composite micromotor by replacing the passive Brownian motor particle with a self-thermophoretic Janus particle, as sketched in Fig. 1. Figure 2(c) depicts the contour plot of the transport velocity of the composite motor. In a wide range of parameters, the composite micromotor drifts along the negative x-direction, similar to

the pure Brownian motor. Nevertheless, the maximum transport velocity of the composite micromotor ($v_{\rm tran} = -0.021$) is larger than that of the Brownian motor. This is mainly because the self-propelled Janus particle can cross more easily the potential barrier region than the passive particle, when the ratchet potential is off.

Interestingly, for small $T_{\rm tot}$ and $T_{\rm on}$, the composite micromotor reverses its transport velocity and drifts toward the slanted edge of the ratchet potential. This reversed transport can be understood based on the following fact: the self-thermophoretic force of the Janus particle ($F_{\rm s} = 1.2$) is much smaller than the external force produced by the steep side of the ratchet potential, but comparable to the strength of the slanted side. Thus the composite micromotor self-propelling along the slanted side of the ratchet potential is dragged back toward the potential minimum only slightly by the short-lived ratchet potential during each on-state. In this case, the persistence length of the active Janus particle ($v_{\rm s}/D_{\rm r} \simeq 4.74$), which is hardly affected due to the weak slanted-side force and the short $T_{\rm on}$, is beyond the length of the slanted side ($L_2 = 4.39$). Thus, the Janus particle has a non-vanishing probability to cross its right-side barrier. In contrast, the active Janus particle cannot surmount its left-side barrier, since the strong force produced by the steep side of the ratchet potential can rapidly drag the Janus particle back to the potential well during each on-state. As a consequence, the composite micromotor displays a weak positive transport in the narrow range of the modulation parameters.

For comparison, we also determine the transport velocity distribution of the active Brownian particle in a time-modulated ratchet potential by Brownian dynamics simulations with the same $v_{\rm s}$, $D_{\rm t}$ and $D_{\rm r}$ as the composite micromotor in the hydrodynamics simulation, as shown in Fig. 2(d). It is found that for small $T_{\rm tot}$ and $T_{\rm on}$ the active Brownian particle can also experience a weak transport along the x-direction, although its transport contour plot is different from that of the composite micromotor.

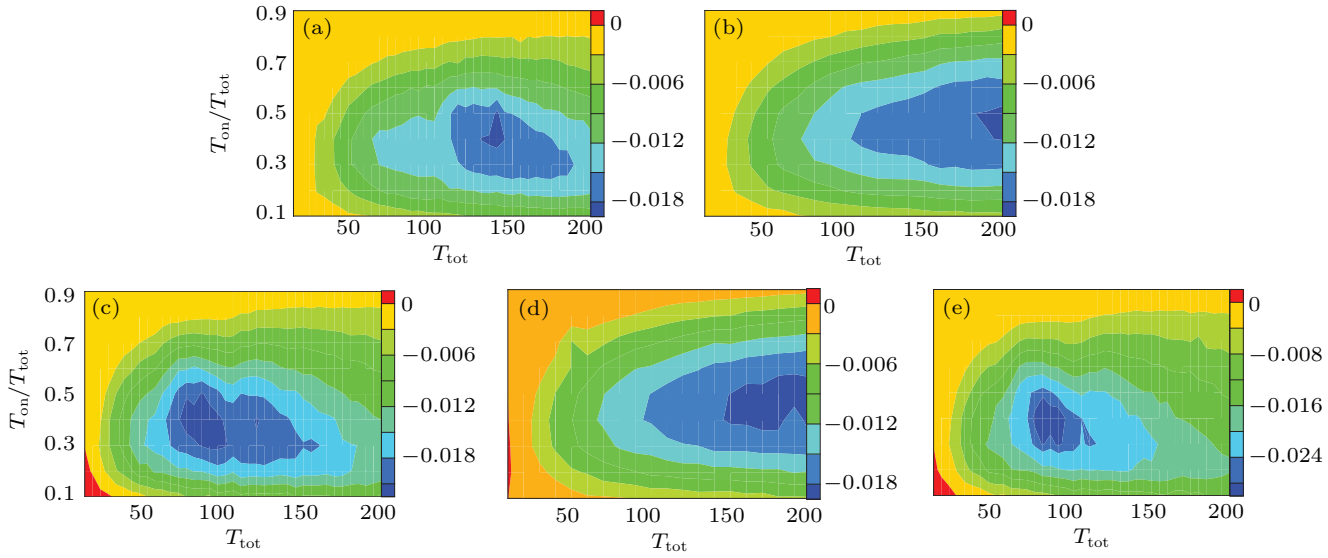


Fig. 2. Contour plots of the micromotor transport velocity in the x-direction as a function of the modulation period $T_{\rm tot}$ and $T_{\rm on}/T_{\rm tot}$. Brownian motor with a passive particle with (a), and without (b) hydrodynamics, (c) composite motor composed of the self-thermophoretic Janus particle, (d) an active Brownian particle moving in a ratchet potential, (e) composite motor with the self-thermophoretic Janus particle having a slip boundary on its non-heated hemisphere. The results in (a), (c), (e) are all obtained by the hybrid mesoscale simulation, while those in (b), (d) are obtained through the Brownian dynamics simulation without explicit solvent.

An important difference between the composite micromotor and the active Brownian particle is reflected by their orientational distributions. The active Brownian particle has a uniform orientational distribution (Fig. 3), as the alignment effect is lacking, while the self-thermophoretic Janus paricle tends to align its heated part towards the steep side of the ratchet potential, as shown in Fig. 3, displaying an inhomogeneous orientational distribution. This alignment is hydrodynamic in its origin. Compared to the non-heated part of the Janus particle, the heat part feels a lower fluid viscosity (weaker friction with the solvent) due to the enhanced temperature. As a result of this asymmetric friction the composite micromotor that transports against the x-direction experiences a (restoring) frictional torque that orients the Janus particle against the x-direction, as sketched in Fig. 1(b). In this situation, the self-thermophoretic direction of the Janus particle is opposite to the transport direction of the composite micromotor.

A natural question thus arises whether we can change the hydrodynamic alignment of the self-thermophoretic Janus particle so as to improve the performance of the composite micromotor. This can be in fact easily achieved by modifying the surface properties of the Janus particle. For instance, when the non-heated surface of the Janus particle is a slip boundary, the anisotropic hydrodynamic friction experienced by the composite micromotor drifting against the x-direction will re-

sult in a restoring frictional torque [Fig. 1(c)], with the stable orientation of the Janus particle pointing along the x-axis, as confirmed by the mesoscale fluid simulation (Fig. 3).

For the Janus particle with its non-heated part having a slip boundary, its stable orientation is thus consistent with the transport direction of the composite micromotor. In this case therefore the hydrodynamic alignment effect will enhance the transport of the composite micromotor. Figure 2(e) plots the transport velocity distribution of such a composite micromotor, displaying a higher maximum transport velocity $v_{\text{tran}} = -0.026$. In addition, this maximum transport velocity is close to the superposition of the self-propelling speed of the pure self-thermophoretic particle and the drift speed of the pure Browmian motor under the same ratchet potential.

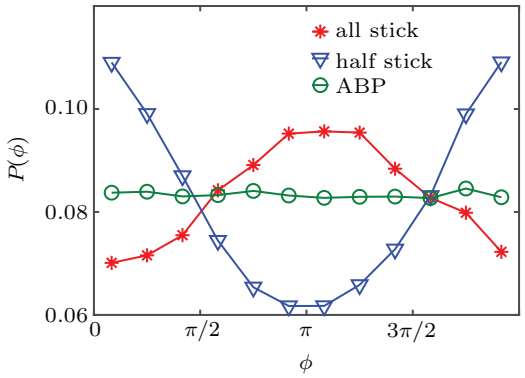


Fig. 3. Orientational probability distribution of different active particles in a ratchet potential, with ϕ the angle between the n and x axes. The simulations are perfomed with $T_{\text{tot}} = 80$ and $T_{\text{on}}/T_{\text{tot}} = 0.4$, for which the particle drifts against the x-direction. The circle refers to the active Brownian particle simulated by the Brownian dynamics method, the cross to the self-thermophoretic particle with the stick surface, and the triangle to the self-thermophoretic particle with the slip boundary for its non-heated part.

4. Conclusion

In this paper, we perform mesoscale dynamics simulations to investigate the transport behaviors of the composite micromotor composed of a self-thermophoretic colloidal particle in a time-modulated ratchet potential. It is found that the composite micromotor exhibits a unidirectional transport, whose direction can be reversed by tuning the modulation frequency of the ratchet potential. Moreover, due to anisotropic surface friction, the active Janus particle exhibits a significant hydrodynamic alignment, in stark contrast to the traditional active Brownian particle. With the alignment effect, the composite motor is able to achieve a maximum transport velocity even close to the superposition of the self-propelling speed of the pure self-thermophoretic particle and the drift speed of the pure Browmian motor. Given the potential applications of self-propelled microswimmers and the ubiquity of thermal fluctuation, our work provides an interesting attempt to actively utilize thermal fluctuations in the performance of microswimmers.

References

[1] Ramaswamy S 2010 *Annu. Rev. Condens. Matter Phys.* **1** 323
[2] Reichhardt C J O and Reichhardt C 2017 *Nat. Phys.* **13** 10
[3] Rubenstein M, Cornejo A and Nagpal R 2014 *Science* **345** 795
[4] Valentini G, Ferrante E, Hamann H and Dorigo M 2016 *Auton Agent Multi-Agent. Syst.* **30** 553
[5] Bricard A, Caussin J B, Desreumaux N, Dauchot O and Bartolo D 2013 *Nature* **503** 95
[6] Morin A, Desreumaux N, Caussin J B and Bartolo D 2017 *Nat. Phys.* **13** 63
[7] Shin J, Cherstvy A G, Kim W K and Metzler R 2015 *New J. Phys.* **17** 113008
[8] Wu W X, Zheng Z G, Song Y L, Han Y R, Sun Z C and Li C P 2015 *Chin. Phys. B* **29** 090503
[9] Lai L, Zhou X X, Ma H and Luo M K 2015 *Acta. Phys. Sin.* **64** 120501 (in Chinese)
[10] Astumian R D 1997 *Science* **276** 917
[11] Van den Broeck C, Kawai R and Meurs P 2004 *Phys. Rev. Lett.* **93** 090601
[12] Hänggi P and Marchesoni F 2009 *Rev. Mod. Phys.* **81** 387
[13] Romanczuk P, Bär M, Ebeling W, Lindner B and Schimansky-Geier L 2012 *Eur. Phys. J. Special Topics* **202** 1
[14] Ghadiri M R, Granja J R and Buehler L K 1994 *Nature* **369** 301
[15] Coy D L, Hancock W O, Wagenbach M and Howard J 1999 *Nat. Cell Biol.* **1** 288
[16] Verhey K J and Hammond J W 2009 *Nat. Rev. Mol. Cell Biol.* **10** 765
[17] Hirokawa N and Noda Y 2008 *Physiol. Rev.* **88** 1089
[18] Carter A P, Garbarino J E, Wilson-Kubalek E M, Shipley W E, Cho C, Milligan R A, Vale R D and Gibbons IR 2008 *Science* **322** 1691
[19] Kardon J R and Vale R D 2009 *Nat. Rev. Mol. Cell Biol.* **10** 854
[20] Huang M, Kapral R, Mikhailov A S and Chen H 2013 *J. Chem. Phys.* **138** 05B613_1
[21] Koyano Y, Kitahata H and Mikhailov A S 2016 *Phys. Rev. E* **93** 022416
[22] Dreyfus R, Baudry J, Roper M L, Fermigier M, Stone H A and Bibette J 2005 *Nature* **437** 862
[23] Howse J R, Jones R A, Ryan A J, Gough T, Vafabakhsh R and Golestanian R 2007 *Phys. Rev. Lett.* **99** 048102
[24] Bechinger C, Di Leonardo R, Löwen H, Reichhardt C, Volpe G and Volpe G 2016 *Rev. Mod. Phys.* **88** 045006
[25] Golestanian R, Liverpool T B and Ajdari A 2007 *New J. Phys.* **9** 126
[26] Jiang H, Yoshinaga N and Sano M 2010 *Phys. Rev. Lett.* **105** 268302
[27] Bregulla A P, Yang H and Cichos F 2014 *ACS Nano* 6542
[28] Xuan M, Wu Z, Shao J, Dai L, Si T and He Q 2016 *J. Am. Chem. Soc.* **138** 6492
[29] Wan M, Reichhardt C J O, Nussinov Z and Reichhardt C 2008 *Phys. Rev. Lett.* **101** 018102
[30] Ghosh P K, Misko V R, Marchesoni F and Nori F 2013 *Phys. Rev. Lett.* **110** 268301
[31] Reichhardt C J O and Reichhardt C 2017 *Annu. Rev. Condens. Matter Phys.* **8** 51
[32] Liao J, Huang X and Ai B 2018 *Soft Matter* **14** 7850
[33] Malevanets A and Kapral R 1999 *J. Chem. Phys.* **110** 8605
[34] Padding J and Louis A A 2006 *Phys. Rev. E* **74** 031402
[35] Kapral R 2008 *Adv. Chem. Phys.* **140** 89
[36] Gompper G, Ihle T, Kroll D M and Winkler R G 2009 *Adv. Polym. Sci.* **221** 1
[37] Ryder J F 2005 *Mesoscopic simulations of complex fluids* (University of Oxford)
[38] Lou X, Yu N, Liu R, Chen K and Yang M 2018 *Soft Matter* **14** 1319
[39] Yu N, Lou X, Chen K and Yang M 2019 *Soft Matter* **15** 408
[40] Yang M, Wysocki A and Ripoll M 2014 *Soft Matter* **10** 6208
[41] Rousselet J, Salome L, Ajdari A and Prostt J 1994 *Nature* **370** 446
[42] Faucheux L P, Bourdieu L, Kaplan P D and Libchaber A J 1995 *Phys. Rev. Lett.* **74** 1504
[43] Bader J S, Hammond R W, Henck S A, Deem M W, McDermott G A, Bustillo J M, Simpson J W, Mulhern G T and Rothberg J M 1999 *Proc. Natl. Acad. Sci. USA* **96** 13165